Available online at www.sciencedirect.com

ScienceDirect

Procedia Engineering 102 (2015) 1436 – 1445

Procedia Engineering

www.elsevier.com/locate/procedia

The 7th World Congress on Particle Technology (WCPT7)

Investigation of Two-Fluid Models of Fluidisation using Magnetic Resonance and Discrete Element Simulations

Xuesong Lu[a], Chris M. Boyce[a], Stuart A. Scott[b], John S. Dennis[a], Daniel J. Holland[a,*]

[a]*Department of Chemical Engineering and Biotechnology, University of Cambridge, Pembroke street, Cambridge CB2 3RA, UK*
[b]*Department of Engineering, University of Cambridge, Trumpington Street, Cambridge CB2 1PZ, UK*

Abstract

The two-fluid model (TFM) coupled with the kinetic theory of granular flow (KTGF) permits detailed simulations of fluidisation at industrial scales in practicable computational time. However, the TFM requires several assumptions regarding the particle-fluid and particle-particle interaction. These models require validation using experimental measurements before the simulations can be used to design industrial fluidised beds. In this paper we present experimental measurements using Magnetic Resonance Imaging (MRI) and compare these with TFM simulations. However, from these experimental comparisons alone, it is difficult to identify whether errors in the TFM arise from the particle-fluid or particle-particle interaction, or both. We therefore explore the origins of any inaccuracies in TFM simulations of fluidised beds using a recently-developed Discrete Element Model coupled with volume averaged Computational Fluid Dynamics (DEM-CFD). The DEM-CFD model is shown to provide accurate predictions of the time averaged velocity of the particulate phase. A comparison of the TFM and DEM-CFD results demonstrates that modelling the particulate phase using an ideal KTGF does not accurately represent the fluidisation behaviour. These errors are attributed to the lack of rotational friction effects in the KTGF. However, by introducing an apparent coefficient of restitution to account for rotation, TFM simulations of the voidage and time-averaged particle velocity agree with the experimental and DEM-CFD results more closely.

Selection and peer-review under responsibility of Chinese Society of Particuology, Institute of Process Engineering, Chinese Academy of Sciences (CAS)

Keywords: Gas-solid fluidisation; Particle velocity; TFM; DEM-CFD; MRI

* Corresponding author. Tel.: +0044-1223-334767.
E-mail address: djh79@cam.ac.uk

Selection and peer-review under responsibility of Chinese Society of Particuology, Institute of Process Engineering, Chinese Academy of Sciences (CAS)
doi:10.1016/j.proeng.2015.01.277

1. Introduction

Computational fluid dynamics (CFD) can potentially be used in the design of industrial-scale fluidised beds; however, models have not yet been sufficiently validated. Up to now, commercial fluidisation processes have largely been designed using empirical correlations and scale-up studies involving pilot-scale equipment. Such an approach is costly, time-consuming and prone to error. CFD provides a tool for modelling the fluidising behaviour of industrial scale reactors and hence potentially permits much more of the detailed design to be performed *in silico*. At present, the most advanced CFD model used for industrial-scale reactors is the two-fluid model (TFM) coupled with the kinetic theory of granular flow (KTGF) [1]. However, the TFM requires several assumptions regarding the particle-fluid and particle-particle interactions, including the premises that (i) the velocities of the particles are Maxwell-Boltzmann distributed, (ii) collisions are only slightly inelastic and described by a constant coefficient of restitution and (iii) that the particle-fluid interaction is governed by a drag model. These two-fluid models, and the underlying assumptions, therefore require further validation before the simulations can be used to design industrial fluidised beds reliably.

The TFM describes the gas and solids motion within a fluidised bed using interpenetrating continua for both the gas and solid phases. In order to describe the solid phase using a continuum model, it is essential to be able to describe the collisions occurring between particles in the particulate phase. The KTGF was introduced to describe the particle phase properties, and TFM simulations incorporating the KTGF have been shown to capture many aspects of fluidisation [2]. Experimental validation of TFMs has most often been performed using relatively simple macroscopic observations of, *e.g.*, the pressure across the bed or expanded bed height and, with certain restrictions, these parameters can be predicted well using the TFM [3]. However, it is unclear if the mesoscopic properties of a fluidised bed, such as the bubble size, bubble rise velocity and the velocities of the particulate phase are accurately described by the TFM. Experimentally, non-invasive imaging techniques such as Magnetic Resonance Imaging (MRI) and Electrical Capacitance Tomography (ECT) are now available to measure these properties, together with granular temperature, [4, 5] in three-dimensional fluidised beds [6]. However, such measurements have not yet been compared with the predictions from TFMs.

One key assumption in the TFM is that the particulate phase is characterized by the so-called "granular temperature", defined in an analogous manner to the temperature of a gas in the kinetic theory of gases. Validation of the granular temperature model used in the TFM is important, because it defines the apparent viscosity and solids pressure in the particulate phase. However, some confusion exists regarding the definition of the granular temperature, Θ, which may be defined as the volume average of the fluctuating component of the particle velocity:

$$\Theta(t) = \frac{1}{3N}\sum_{k=1}^{3}\sum_{i=1}^{N}\left(v_{p,k}^{i}(t) - \overline{v_{p,k}}(t)\right)^2 \tag{1}$$

where N is the number of particles in the cell, $v_{p,k}^{i}$ is the velocity of the ith particle in the kth direction and

$$\overline{v_{p,k}}(t) = \sum_{i=1}^{N} v_{p,k}^{i} \Big/ N \tag{2}$$

This definition arises naturally from the volume averaging used to derive the continuum model [7]. Experimental measurements of Θ are difficult to obtain, especially in dense opaque systems, such as a fluidised bed. This has given rise to an alternative definition of the granular temperature, the bubble granular temperature, Θ_b, which characterizes temporal fluctuations in the average velocity [9]:

$$\Theta_b(t) = \frac{1}{3T}\sum_{k=1}^{3}\sum_{t=1}^{T}\left(\overline{v_{p,k}}(t) - V_k\right)^2 \tag{3}$$

where T is the number of discrete observations of the average velocity of the particles, and

$$V_k = \sum_{i=1}^{T}\overline{v_{p,k}}(t) \Big/ T \tag{4}$$

Although Θ_b is not a measure of the granular temperature as defined in Eq. 1, it is more readily accessible experimentally. The granular temperature has been measured using optical techniques [9] and acoustic noise [10], a hybrid of bubble and particle granular temperature has been measured using MRI [4].

The discrete element method coupled with computational fluid dynamics (DEM-CFD) provides a useful tool for validating the TFM [11, 12]. The DEM-CFD method tracks the motion of all the particles in the system. Due to limitations of computer hardware, the number of particles that can be tracked is typically limited to ~10^6 and therefore it is not possible currently to use DEM-CFD for simulations at the industrial scale. However, DEM-CFD can model the particle-particle interaction more accurately than the TFM and therefore presents a useful tool to study fundamental aspects of granular flows, and in particular the assumptions inherent in TFM simulations. Particle-particle interaction in DEM-CFD can be modelled using a hard-sphere or soft-sphere approach [13]. Hard-sphere models permit only single particle contacts at a time, but are computationally efficient [14]. Soft-sphere approaches permit contacts among multiple particles but require more complicated and computationally-intensive equations to describe the collisions [15]. Both soft-sphere and hard-sphere approaches have been shown to characterize the fluidisation dynamics [16, 17]**.** According to the number of particle-particle interactions in a given time, the simulations can be classified into three categories: collision-free flow (dilute phase flow); collision-dominated flow (medium concentration flow) and contact-dominated flow (dense phase flow) [18]. In contact-dominated flow, the rotation of the particles strongly influences the flow of particles [19]. Particle rotation also plays a dominant role in the development of shear bands [20]. In collision-dominated flow, the relative rotation between contacting particles or between a particle and a wall will produce a rolling resistance due to the resulting elastic hysteresis loss [21]. Sometimes, the rolling resistance can be very large if particles undergo an internal circulating flow [21]. These findings indicate that the rotation of particles can provide a means for the dissipation of energy in granular flows.

Lu et al. [11] used DEM-CFD to investigate the KTGF by calculating the normal stress and shear stress from DEM-CFD simulations. The results showed that the effective particle pressure obtained from the DEM-CFD simulations was of similar magnitude to that calculated from the KTGF, but that the apparent viscosity of the solid phase was significantly less than that predicted by the KTGF. Numerical results were not compared with experimental measurements in this study. Goldschmidt et al. [12] compared a hard-sphere DEM-CFD model with TFM simulations and experimental measurements of the bubble shape, time-averaged particle velocity and bed expansion. They concluded that the DEM-CFD model more accurately represents the fluidisation dynamics than the TFM and attributed the difference in behaviour to the effect of particle rotation, which is ignored in the KTGF. However, Goldschmidt et al.'s [12] experimental measurements were restricted to optical observations of particles in a thin, pseudo two-dimensional bed, and it is well known that the fluidisation behaviour of two-dimensional beds is distinctly different from that of three-dimensional beds, e.g., [22], even at a small scale. Therefore, although the KTGF is a fair approximation of the behaviour of the particulate phase in a fluidised bed, it does not completely represent the behaviour of the particulate phase.

In this paper, we compare TFM and DEM-CFD simulations with experimental measurements of the time-averaged particle velocity and granular temperature in a fluidised bed obtained using MRI. The DEM-CFD simulations and experiments are used to investigate the effect of particle rotation, friction, and granular temperature modelling on the TFM simulations.

2. Experiment

Experimental observations were made on a fluidised bed contained in an acrylic tube (i.d. 44 mm. o.d. 60 mm) with a porous glass frit (i.d. 40 mm) as the gas distributor. Rhoeas poppy seeds were the particles fluidised (particle size: d_p =1.2 mm; particle density: ρ_s = 900 kg m^{-3}; experimentally measured minimum fluidisation velocity: U_{mf} = 0.3 m s^{-1} at STP). The initial settled bed height was 30 mm. The bed was fluidised by humidified air at ambient temperature and pressure at $2U_{mf}$. The solids velocity was measured by magnetic resonance imaging using a Bruker DMX 200 spectrometer operating in the vertical orientation at a proton (^{1}H) frequency of 199.7 MHz. For a single measurement of the axial component of the time-averaged velocity of the particles, the acquisition time was 2 hours. Full experimental details are given elsewhere [5].

3. Theory

3.1 TFM.

The TFM is based on the Navier-Stokes equations in which both the fluid and solids phases are treated as continua occupying the same space. Thus, it has two hydrodynamic equation sets, one for each phase, and additional equations are used to describe the interaction between the phases. For the solids phase, the solids pressure and viscosity were determined by the KTGF. Frictional stresses were either ignored or modelled by either the Schaeffer model [23] or the Princeton model [24]; unless otherwise specified, the Princeton model was used. The granular temperature in the fluidised bed was estimated using either the full partial differential transport equation, or a simplified algebraic model. The algebraic model assumes that the granular temperature is in a pseudo-steady state such that the granular temperature in any cell is a balance of the local generation and dissipation terms in the full model. The drag model developed by Beetstra et al. [25] was used to describe the interaction between the gas and solids phase. In this work, the open-source MFIX (Multiphase Flow with Interphase eXchanges CFD code) developed by National Energy Technology Laboratory (NETL) USA was used. The 2nd order superbee scheme was used to discretize the governing equations. A semi-implicit scheme with automatic time-step adjustment was used to reduce the simulation time. A 3D mesh based on cylindrical coordinates with dimensions 11(r) × 12(θ) × 30(z) was used to represent a real-space geometry of diameter 44 mm and length 100 mm. The equations of TFM in MFIX are described in detail elsewhere [26]. The superficial velocity for the gas phase was 0.6 m s^{-1}. Since the porous frit used in the experiments was 40 mm in diameter, to achieve the correct superficial velocity in the TFM simulation, the gas superficial velocity at the distributor was set to 0.726 m s^{-1} in the 10 cells in the centre of the bed and 0 m s^{-1} for the outermost cell of the grid. The coefficient of restitution for the particulate phase was initially set to 0.93. The simulations were run for 20 s of real time. Time-averaged results were obtained from the final 10 s of the simulation by averaging the velocity or granular temperature of the particulate phase, as appropriate, every 0.01 s.

3.2 DEM-CFD.

The DEM-CFD model has been described elsewhere [27]. Newtonian physics and contact mechanics are used to simulate the motion of each individual particle in the fluidised bed and the volume averaged Navier-stokes equation is used to simulate the continuum fluid phase. A soft-sphere collision model is used. The normal contact force was determined using a Hertzian model and the tangential contact force was determined by the model of Tsuji et al. [28]. Coulomb's law was introduced to account for sliding. The particles were modelled such that the coefficient of restitution in a normal collision was 0.93. The drag force of interaction between fluid and particles was modelled using the drag law developed by Beetstra et al. [25]. The particle and fluid motion were stepped forward explicitly in time using the 3rd order Adams-Bashforth scheme. An explicit scheme was used to allow for pressure waves to travel through the system and the 3rd order Adams-Bashforth scheme was used to increase simulation accuracy and stability as compared with first- and second-order time stepping techniques. The fluid was modelled in 3-D cylindrical coordinates and the motion of particles was modelled in 3-D rectangular coordinates.

4. Results

4.1. Comparison of TFM and DEM-CFD simulations with MRI measurements

Figure 1 shows a comparison of TFM and DEM-CFD simulations with MRI measurements of the particle velocity in the fluidised bed at a superficial gas velocity of 2U_{mf}. The TFM simulations show a qualitatively similar time-averaged particle velocity distribution to that obtained experimentally, with particles rising in the centre of the bed and falling at the walls in a classic gulf-streaming flow pattern. However, the maximum time-averaged velocity predicted by the TFM is only 0.17 m s^{-1}, compared with 0.31 m s^{-1} measured using MRI. On the other hand, the DEM-CFD model accurately predicted the time-averaged particle velocities, both qualitatively and quantitatively. The maximum velocity obtained from the DEM-CFD model was 0.31 m s^{-1}, in good agreement with that determined experimentally. The only region of the bed in which the DEM-CFD model failed to predict accurately the velocity of the particles is near the top of the bed, where the predicted velocity was approximately 67 % of that measured experimentally. This discrepancy might be due to a difference in the expanded bed height, perhaps arising from

inaccuracies in the drag law used [29]. Since the majority of the fluidised bed is accurately simulated using DEM-CFD, it is reasonable to use these results to investigate the assumptions used in the TFM.

Figure 2 shows the time-averaged granular temperature obtained from the MRI measurements, and the TFM and DEM-CFD simulations for the same conditions as that used in Figure 1. Experimentally it is challenging to measure the true granular temperature, Θ, and therefore the granular temperature shown here is Θ_b [6]. An estimate of Θ_b was obtained from the DEM-CFD simulations by calculating the variance from the time-averaged velocity of all particles at a given spatial location, a method which closely approximates the experimental measurement. For the TFM, the bubble granular temperature was calculated from the temporal fluctuation in the average particle velocity. The method for calculating the Θ_b from the TFM is designed to approximate the experimentally-measured value as closely as possible; however, some discrepancies may remain. The magnitude of Θ_b in the TFM simulations in Figure 2(b) is significantly lower than the experimentally-measured values shown in Figure 2(a), consistent with the lower particle velocity observed in Figure 1. On the other hand, Θ_b in the DEM-CFD simulations is comparable to that obtained experimentally, although the observed pattern differs with the DEM-CFD model showing significantly greater values of granular temperature at the walls in the dense region of the bed. Although the quantitative agreement between the DEM-CFD and the experiments is not perfect, the results are still sufficiently close for it to be reasonable to use the DEM-CFD model to investigate some of the assumptions inherent in the TFM simulations.

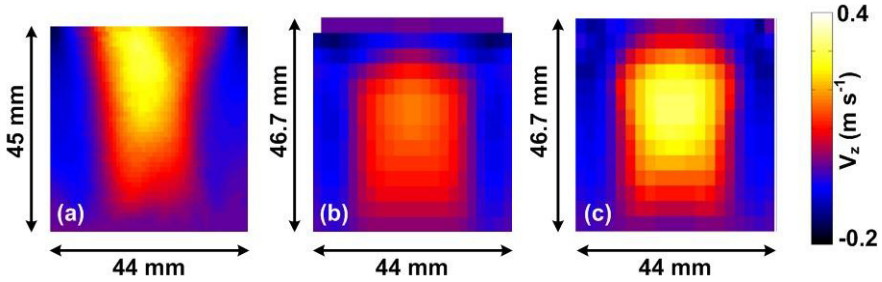

Fig. 1. Time averaged vertical particle velocity obtained from (a) MR experiment, (b) TFM simulation (e = 0.93) and (c) DEM-CFD simulation.

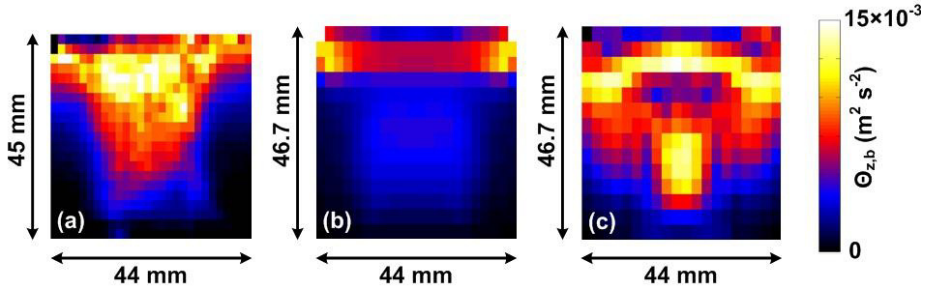

Fig. 2. Time-averaged bubble granular temperature obtained from (a) MR experiment, (b) TFM simulation (e = 0.93) and (c) DEM-CFD simulation.

4.2. Consideration of particle rotation

Previously, differences between TFM and DEM-CFD simulations have been attributed to the effect of particle rotation [12]. The TFM with the KTGF does not account for any tangential or sliding friction, and therefore the particles are effectively prevented from rotating in this model. In Figure 3, the effect of the rotation of the particles is illustrated by calculating the effective coefficient of restitution resulting from the collision of two spherical particles using our DEM-CFD model as a function of the vertical offset between the centre of the two 1.2 mm diameter particles. For the case shown in Figure 3, with the second sphere initially stationary, we define an effective coefficient of restitution as the ratio of the translational speed of the particles before and after collision, *i.e.*:

$$e_{\text{eff}} = \frac{\left|v_{1,f} - v_{2,f}\right|}{\left|v_{1,i}\right|} \tag{5}$$

where $v_{k,i}$is the velocity of the kth particle before collision and $v_{k,f}$ is the velocity of the kth particle after collision. The fluid phase was not included in these simulations. For collisions that are close to the central axis of the two particles, i.e. with a vertical offset < 0.2 mm, the coefficient of restitution is constant at a value of ~0.93. However, as the offset between the two particles increases, rotational effects become more significant and some of the energy of the particles prior to collision is transferred to rotational motion of the particles and is lost from the translational motion. The effective coefficient of restitution therefore decreases, reaching a minimum at an offset of approximately 0.8 mm. For glancing collisions, the energy absorbed by the particles during the collision decreases and the coefficient of restitution approaches 1. Similar values for e were obtained, regardless of the initial velocity and initial rotation of the particle.

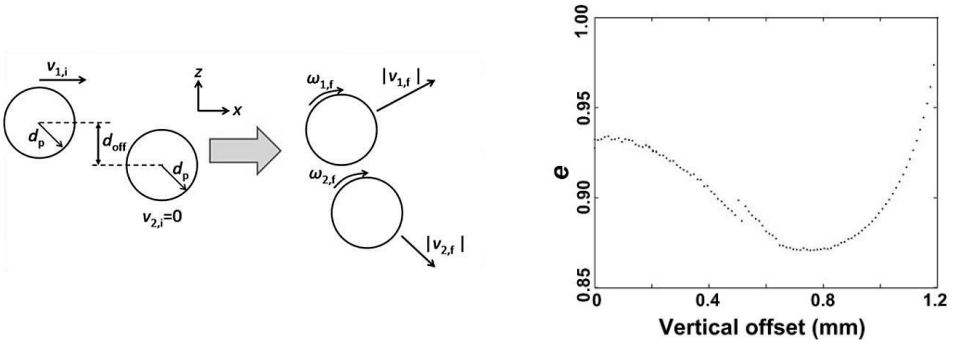

Fig. 3. Schematic diagram of (a) a two-ball collision model and (b) the apparent coefficient of restitution as a function of the vertical offset between the two balls. The effective coefficient of restitution is calculated from the change in the magnitude of the momentum following collision. (v_i = 0.5 m/s; $w_{i,z}$ = 150 rad/ s; d_p = 1.2 mm). The slight discontinuity at an offset of ~0.5 mm corresponds to the transition from sticking to sliding friction.

Goldschmidt et al. [12] observed the effect of rotation on the apparent coefficient of restitution and introduced an effective coefficient of restitution to their TFM simulations, based on the collision model of Jenkins and Zhang [30], to account for the effect of rotation of the particles. They related the effective coefficient of restitution (e_{eff}) to the coefficient of normal restitution (e_n), coefficient of tangential restitution (β_0), and the dynamic coefficient of friction (μ). The value of μ for poppy seeds is ~ 0.4 [31, 32], so, according to the equations given by Goldschmidt et al. [12], e_{eff} ~ 0.70 and is largely independent of the coefficient of tangential restitution. However, the simulations shown in Figure 3 suggest that e_{eff} is somewhat larger than this, as the minimum of the calculated coefficient of restitution is approximately 0.87.

Accordingly, the TFM simulations shown in Figure 1 were repeated with an effective coefficient of restitution of either e = 0.87 or e = 0.7. At the same time, the DEM-CFD simulations were repeated with all rotational forces set to zero to provide a comparison for the TFM simulations with e = 0.93. The results of these simulations are shown in Figure 4. The DEM-CFD simulations with rotation turned off, Figure 4a, show significantly lower time-averaged particle velocities than those observed with particle rotation. The maximum time-averaged particle velocity from these simulations was 0.21 m s^{-1}, approaching that of 0.17 m s^{-1} obtained from the TFM simulations with e = 0.93. Thus, the DEM-CFD simulations in which particle rotation is not included are consistent with the TFM simulations, as also shown by Goldschmidt et al. [12]. Lowering the effective coefficient of restitution in the TFM simulations to 0.87 results in a higher time-averaged particle velocity, as shown in Figure 4b. For the TFM simulations, the maximum time-averaged particle velocity was 0.25 m s^{-1} for e = 0.87, approaching the maximum particle velocity of 0.31 m s^{-1} obtained from the DEM-CFD simulation with rotation, and that measured experimentally. Further decreasing the effective coefficient of restitution resulted in a small decrease in the averaged particle velocity and a significant reduction in the width of region in which particles are travelling upwards, as seen in Figure 4c.

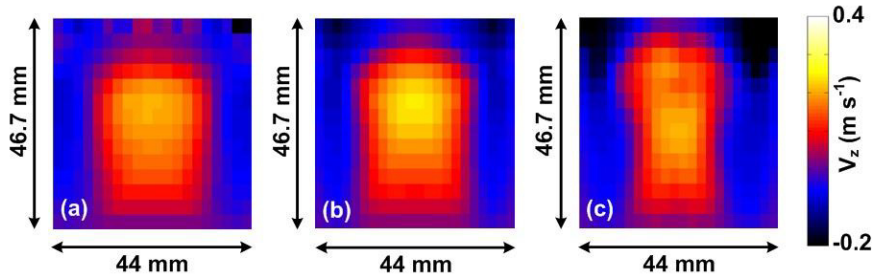

Fig. 4. Time-averaged vertical particle velocity obtained from (a) DEM-CFD simulation without rotation, (b) TFM simulation (e = 0.87) and (c) TFM simulation (e = 0.70).

Figure 5 shows the bubble granular temperature obtained from the simulations used to generate Figure 4. The DEM-CFD simulations with no rotation, Figure 5a, show that the bubble granular temperature is approximately constant over the cross section of the bed, whereas the TFM simulations with e = 0.93, Figure 2(b), show a significant increase in the granular temperature in the centre of the bed. Despite this variation, the magnitude of the bubble granular temperature in both simulations is consistent, again highlighting the importance of the rotational effects on the particle motion in the bed. The TFM simulations with e = 0.87 and 0.7 result in significantly greater bubble granular temperatures than those observed with e = 0.93. The distribution of bubble granular temperatures with e = 0.7 is larger than that observed experimentally. With e = 0.87, the magnitude of the bubble granular temperature is closer to that observed experimentally, although the values are still somewhat lower than those given by the DEM-CFD (with rotation) and by MRI measurement. These results support the idea that reducing the coefficient of restitution in TFM helps to account for the effect of rotation; however, they also suggest that additional factors may also apply.

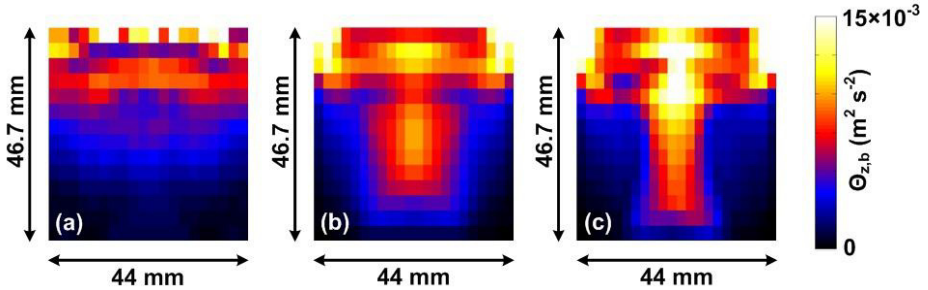

Fig. 5. Vertical component of the bubble granular temperature obtained from (a) DEM-CFD simulation without rotation, (b) TFM simulation (e = 0.87) and (c) TFM simulation (e = 0.70).

4.3. TFM simulation with and without frictional stress

Granular flow can be classified into two distinct flow regimes: a viscous rapid-shear regime in which stresses arise because of collisional or translational transfer of momentum, and a plastic or slow-shear regime, in which stresses arise because of friction between particles in enduring contact [34]. In TFM simulations, collisional stresses are modelled using the KTGF whilst frictional stress is typically modelled using theory developed for soil mechanics [24]. However, there is uncertainty over the best approach for modelling frictional stresses in TFM simulations. Here, TFM simulations with no frictional stress are compared with the frictional stress model of Schaeffer et al. [23] (Schaeffer model) and that of Srivastava and Sundaresan [24] (Princeton model). The Schaeffer model is for quasi-static flow and is strictly valid only at the critical state where the granular assembly deforms without any change in volume. The Princeton model accounts for strain-state fluctuations and slow relaxation of the assembly to the yield surface and hence includes volume changes during deformation [24]. The time-averaged particle velocities obtained with all three of these simulations were found to be nearly identical, and therefore these results are not shown.

Instead to compare the simulations using different frictional stress models, Figure 6 shows the distribution of time-averaged true granular temperature Θ within the fluidised bed. When a model with no frictional stress is used, the granular temperature in the centre of the fluidised bed is significantly greater than that seen when either of the frictional stress models are used; there was no observable difference in the distribution of the granular temperature obtained using the Schaeffer model and the Princeton model. Furthermore, the distributions of granular temperatures obtained from the TFM simulations that include a frictional stress model are in good agreement with the distribution obtained from the DEM-CFD simulations, as shown in Figure 6(a). These results indicate that it is important to model the frictional stress when simulating bubbling fluidised beds with the TFM, as shown by others [24]. The Schaeffer model has the advantage for this system, being computationally simpler than the Princeton model.

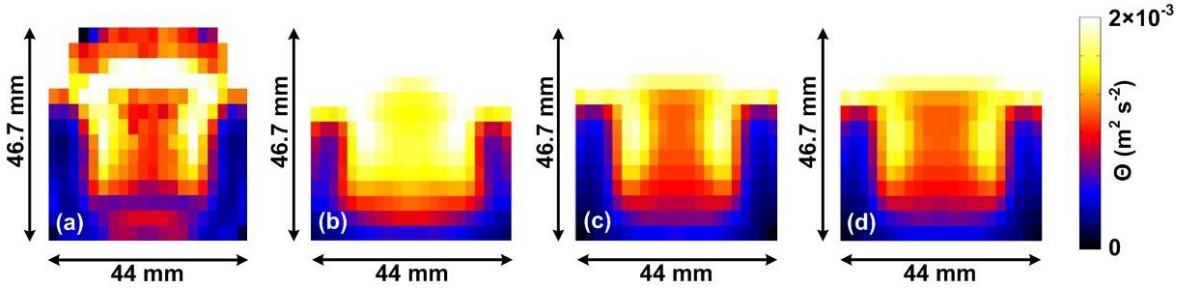

Fig. 6. True granular temperature obtained from (a) DEM-CFD, (b) TFM simulation (e = 0.87) without frictional stress, (c) TFM simulation (e = 0.87) with the Schaeffer model for frictional stress and (d) TFM simulation (e = 0.87) with the Princeton model for frictional stress.

4.4. TFM simulation with full transport equation and local dissipation equations of granular temperature

A key parameter in TFM simulations is the granular temperature, because it determines the effective pressure and viscosity of the particulate phase. In the TFM, the granular temperature is calculated as an independent variable for the particulate phase with a partial differential equation describing the generation, dissipation and transport of the granular temperature (PDE model). It is common practice to simplify TFM calculations by using a pseudo-steady state assumption for the granular temperature, in which the granular temperature at any location within the bed is simply determined by the balance between the generation and dissipation terms [28]. This simplification means that the granular temperature can be described by an algebraic equation, because transport of the granular temperature is assumed to be negligible (algebraic model). Figure 7 shows the time-averaged particle velocity obtained from the TFM simulations using both the full PDE form of the granular temperature model and the simplified algebraic form; in both cases e = 0.87 was used with the Schaeffer model for frictional stress. The time-averaged velocities resulting from these simulations are quite similar; however, the algebraic form of the granular temperature model produces a central core with a narrow base widening towards the top of the bed. The time-averaged particle velocities using the algebraic model are larger than those obtained using the PDE model for the granular temperature. The velocities obtained from the algebraic model are similar to those measured experimentally (~0.30 m s^{-1}), whilst the velocities obtained from the full PDE model are lower (0.25 m s^{-1}). These results suggest that perhaps it would be better to use the simplified, algebraic model for the granular temperature when modelling the fluidised bed.

To investigate these assumptions further, a distribution of granular temperature was calculated from the DEM-CFD model and compared with that obtained from the TFM. In this case, the true granular temperature was considered and therefore it cannot be compared with the results of experiments. The resulting distributions of granular temperature from the TFM and DEM-CFD are shown in Figure 8. The DEM-CFD results indicate that the granular temperature is approximately 1 to 2 × 10^{-3} m^2 s^{-2} throughout the region of the central core. This is in broad agreement with the value obtained from the TFM when using the PDE model of the granular temperature. However, the TFM simulations using the algebraic form of the granular temperature model produced significantly larger values in the core region, often > 2 × 10^{-3} m^2 s^{-2}, whilst the granular temperature approached zero towards the walls. Therefore, although the time-averaged velocities are similar, the DEM-CFD results indicate that it is not justified to use the algebraic form of the granular temperature in a bubbling fluidised bed, and that the pseudo-steady state simplification is invalid, as expected.

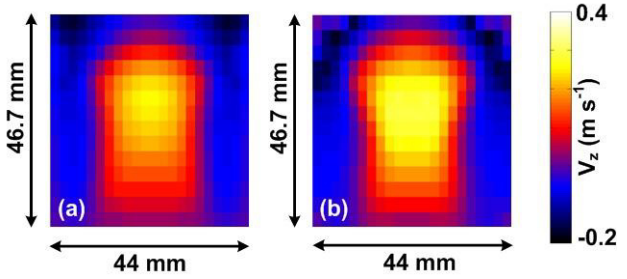

Fig. 7. Time-averaged vertical particle velocity obtained from the TFM simulation (e = 0.87) using (a) pde model for the granular temperature and (b) the algebraic, or pseudo-steady state, model for the granular temperature. In both cases the Schaeffer model for frictional stress was used.

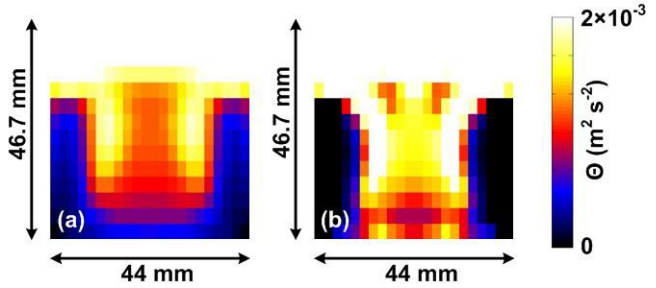

Fig. 8 True granular temperature obtained from (a) TFM simulation (e= 0.87) using the pde model for the granular temperature and (b) TFM simulation (e = 0.87) using the algebraic model for the granular temperature. In both TFM simulations the Schaeffer model was used for frictional stress.

5. Conclusions

This research compares two approaches to modelling a bubbling fluidised bed, using either TFMs or DEM-CFD, with experimental observations. The DEM-CFD simulations were found to be in good agreement with the MRI experiments, indicating that the DEM-CFD model could be used for a more detailed analysis of the TFM. The TFM was found to underpredict the time-averaged particle velocity measured by MRI. By comparison with DEM-CFD simulations, it was concluded that the major reason for this discrepancy was the effect of particle rotation which is not included in the conventional KTGF closure model used to characterize the particle phase. The TFM can approximate the behaviour of the fluidised bed more accurately if an apparent coefficient of restitution is introduced to characterize the dissipation of kinetic energy arising from tangential frictional forces occurring during collisions of particles. Finally, the importance of incorporating a frictional stress model for the particle phase was demonstrated by comparison of the granular temperature predicted from the TFM and the DEM-CFD simulations. If either the Schaeffer or Princeton model for the frictional stresses is used, the granular temperature distribution obtained from the TFM simulations shows good agreement with the DEM-CFD simulations.

Acknowledgements

The authors would like to acknowledge the National Energy Technology Laboratory (NETL) of the USA for providing the MFIX two fluid model used in this work. Financial support was provided by the Engineering and Physical Sciences Research Council (EPSRC) under grant EP/K008218/1. CMB would like to acknowledge financial support from the Gates Cambridge Trust.

References

[1] D.Gidaspow, J. Jung, R.K. Singh, Hydrodynamics of fluidisation using kinetic theory: an emerging paradigm: 2002 Flour-Daniel lecture, Powder Technol. 148 (2004) 123-141.

[2] J. Ding, D. Gidaspow, A bubbling fluidisation model using kinetic theory of granular flow, AIChE J. 26 (1990) 523-538.

[3] F. Taghipour, N. Ellis, C. Wong, Experimental and computational study of gas-solids fluidised bed by dynamics, Chem. Eng. Sci. 60 (2005) 6857-6867.

[4] D.J. Holland, Q. Marashdeh, C.R. Müller, F. Wang, J.S. Dennis, L.-S. Fan, L.F. Gladden, Comparison of ECVT and MR measurements of voidage in a gas-fluidised bed, Ind. Eng. Chem. Res. 48 (2009) 172-181.

[5] D.J. Holland, C.R. Müller, J.S. Dennis, L.F. Gladden, A.J. Sederman, Spatially resolved measurement of anisotropic granular temperature in gas-fluidised beds, Powder Technol. 182 (2008) 171-181.

[6] C.R. Müller, D.J. Holland, A.J. Sederman, S.A. Scott, J.S. Dennis, L.F. Gladden, Granular temperature: comparison of magnetic resonance measurements with discrete element model simulations, Powder Technol. 184 (2008) 241-253.

[7] T.B. Anderson, R. Jackson, Fluid mechanical description of fluidised beds. Equations of motion, Ind. Eng. Chem. Fundamen. 6 (1967) 527-539.

[8] R.D. Wildman, J.M. Huntley, D.J. Parker, Granular temperature profiles in three-dimensional vibrofluidised granular beds, Phy, Rev. E 63 (2001) 061311.

[9] J. Jung, D. Gidaspow, Measurement of two kinds of granular temperatures, stresses and dispersion in bubbling beds, Ind. Eng. Chem. Res. 44 (2005) 1329-1341.

[10] G.D. Cody, D.J. Goldfarb, G.V. Storch, A.N. Norris, Particle granular temperature in gas fluidised beds, Powder Technol. 87 (1996) 211-232.

[11] H. Lu, S. Wang, Y. Zhao, L. Yang, D. Gidaspow, J. Ding, Prediction of particle motion in a two-dimensional bubbling fluidised bed using discrete hard-sphere model, Chem. Eng. Sci. 60 (2005) 3217-3232.

[12] M.J.V. Goldschmidt, R. Beetstra, J.A.M. Kuipers, Hydrodynamic modeling of dense gas-fluidised beds: comparison and validation of 3D discrete particle and continuum models, Powder Technol. 142 (2004) 23-47.

[13] N.G. Deen, M. Van S. Annaland, M. A. Van der Hoef, J.A.M. Kuipers, Review of discrete particle modeling of fluidised beds, Chem. Eng. Sci. 62 (2007) 28-44.

[14] B.P.B. Hoomans, J. A.M. Kuipers, W.J. Briels, W.P.M. van Swaalij, Discrete particle simulation of bubble and slug formation in a two-dimensional gas-fluidised bed: a hard-sphere approach, Chem. Eng. Sci. 51 (1996) 99-118.

[15] V. Suryawanshi and S. Roy, DEM simulation of gas-solids circulating fluidised beds, J. Chem. Eng. Jpn. 42 (2009) s130-s136.

[16] T. Li, C. Guenther, MFIX-DEM simulations of change of volumetric flow in fluidised beds to chemical reactions, Powder Technol. 220 (2012) 70-78.

[17] Y. He, T. Wang, N. Deen, M. van S. Annaland, H. Kuipers, D. Wen, Discrete particle modeling of granular temperature distribution in a bubbling fluidised bed, Particuol. 10 (2012) 428-437.

[18] Y. Tsuji, Activities in discrete particle simulation in Japan, Powder Technol. 113 (2002) 278-286.

[19] H. Teufelsbauser, Y. Wang, S.P. Pudasaini, R.I. Borja, W. Wu, DEM simulation of impact force exerted by granular flow on rigid structures, Acta Geotechnica 6 (2011) 119-133.

[20] K. Iwashita, M. Oda, Rolling resistance at contacts in simulation of shear band development by DEM, J. Eng. Mech. 124 (1998) 285-292.

[21] X.L. Zhao, S.Q. Li, G.Q. Liu, Q. Yao, J.S. Marshall, DEM simulation of the particle dynamics in two-dimensional spouted beds, Powder Technol. 184 (2008) 205-213.

[22] D. Geldart, The size and frequency of bubbles in two- and three- dimensional gas-fluidised beds, Powder Technol. 4 (1970) 41-55.

[23] D.G. Schaeffer, E. B. Pitman, Ill-posedeness in three-dimensional plastic flow, Comm. Pure Appl. Math. 41(1988) 879-890

[24] A. Srivastava, S. Sundaresan, Analysis of a frictional-kinetic model for gas-particle flow, Powder Technol. 129 (2003) 72-85.

[25] R. Beetstra, M.A. van der Hoef, J.A.M. Kuipers, Drag force of intermediate Reynolds number flow past mono- and bidisperse arrays of spheres, AIChE J. 53 (2007) 489-501.

[26] S. Benyahia, M. Syamlal, T.J. O'Brien, Summary of MFIX equations 2012-1, https://mfix.netl.doe.gov/documentation / MFIXEquations2012-1.pdf, January 2012.

[27] C.M. Boyce, D.J. Holland, S.A. Scott, J.S. Dennis, Adapting data processing to compare model and experiment accurately: a discrete element model and magnetic resonance measurements of a 3D cylindrical fluidised bed, Ind. Eng. Chem. Res. Submitted, (2014).

[28] Y. Tsuji, T. Tanaka, T. Ishida, Lagrangian numerical simulation of plug flow of cohesionless particles in a horizontal pipe, powder Technol. 71 (1992) 239-250.

[29] C.M. Boyce, D.J. Holland, S.A. Scott, J.S. Dennis, Adapting data processing to compare model and experiment accurately: a discrete element model and magnetic resonance measurements of a 3D cylindrical fluidised bed. Ind. Eng. Chem. Res. 52 (2013) 18085–18094.

[30] J.T. Jenkins, C. Zhang, Kinetic theory for identical, frictional, nearly elastic spheres, Phys. Fluids, 14 (2002), 1228-1235.

[31] C. Li, T. Zhang, D.I. Goldman, A terradynamics of legged locomotion on granular media, Science 339 (2013) 1408-1412

[32] Y.F. Sharobeem, Apparent dynamic friction coefficients for grain crops, Misr. J. Ag. Eng. 24 (2007)557-574.

[33] V. Verma, N.G. Deen, J.T. Padding, J.A.M. Kuipers, Two-fluid modelling of three dimensional cylindrical gas-solid fluidised beds using the kinetic theory of granular flow, Chem. Eng. Sci. 102 (2013) 227-245

[34] M. Syamlal, W. Rogers, T.J. O'Brien, MFIX documentation theory guide, DOE/METC-94/1004 (DE94000087), US Department of Energy, Morgantown, West Virginia, US, December 1993.